Langmuir

Revised

1 October 2012

Electrical Behavior of Langmuir-Blodgett Networks of Sorted Metallic and Semiconducting Single-Walled Carbon Nanotubes

Mark K. Massey, Mark C. Rosamond, Christopher Pearson, Dagou A. Zeze, Michael C. Petty

School of Engineering and Computing Sciences and Centre for Molecular and Nanoscale Electronics, Durham University, South Road, Durham, DH1 3LE

Abstract

Langmuir-Blodgett deposition has been used to form thin film networks of both metallic and semiconducting single-walled carbon nanotubes. These have been investigated to understand their physical, optical and morphological properties. The electrical conductivities over the temperature range 80 K to 350 K and across electrode gaps of 220 nm and 2 mm have been explored. In the case of semiconducting tubes, the results suggest that Poole-Frenkel conduction is the dominant electrical process at temperatures below 150 K and electric fields of greater than 1 MV m^{-1}. Metallic nanotube networks exhibit a decrease in resistance with a reduction in temperature. This can be approximated by a linear relationship, giving a temperature coefficient of resistance of 10^{-3} K^{-1}.

Introduction

Carbon nanotubes (CNTs) are generating enormous interest as a potential new material for applications in electronics. For example, thin films of CNTs may be useful as transparent conducting electrodes or as the active layer in chemical sensors or thin film transistors. The films can be deposited by direct growth methods, however solution based processing techniques are favored. The lower temperature processes not only provide reduced energy costs, but also allow coating onto a variety of flexible (e.g. plastic) substrates.[1]

The Langmuir-Blodgett (LB) technique is a simple and elegant means of building up multilayer architectures of amphiphilic compounds. Although CNTs are not inherently amphiphilic, there are a number of reports of LB deposition of these materials.[2,3] Often, nanotubes are dispersed with amphiphilic polymers in organic solvents to improve dispersion[4] or the nanotubes are chemically modified to improve their solubility.[5] This research builds on our previous work[6,7] in which we used the LB technique to fabricate thin films of unsorted CNTs (i.e. containing a mixture of metallic and semiconducting nanotubes). Here, we describe a study of the LB deposition of undiluted and unmodified metallic and semiconducting nanotubes, and compare the morphologies of the different films. Furthermore, we report detailed electrical conductivity data for these layers. The effects of electrode spacing and temperature are used to elucidate the dominant physical processes in the thin film networks.

Experimental Methods

Sorted single-walled carbon nanotubes (SWCNTs) were obtained from NanoIntegris in dried mat form. The unsorted material was separated by NanoIntegris by density gradient ultracentrifugation into semiconducting (SWCNT-S) and metallic nanotubes (SWCNT-M).[8]

The purity of the sorted material was 98 % for semiconducting nanotubes and 95 % for metallic. For both types of nanotube, catalyst impurities were approximately 1 % and carbonaceous impurities were below 5 %. The metallic or semiconducting SWCNTs were dispersed in chloroform (Fisher Scientific, 99.9 % purity) by ultrasonication to a concentration of ~0.02 mg ml^{-1}. No additional surfactants were added to either solution. Both materials contained nanotubes with a mean diameter of 1.4 nm. The mean tube length was approximately 1 μm for the semiconducting material and about 0.5 μm in the case of the metallic nanotubes.

A Molecular Electronics LB715 trough situated in a class 10,000 cleanroom was used to record surface pressure versus area isotherms and to perform LB deposition. A pure water subphase was used, with the addition of varying percentages (by volume) of methanol (Fisher Scientific, analytical reagent grade) to reduce the surface tension of the water. The water was purified by reverse osmosis, followed by carbon filtration, two stage deionisation and UV sterilisation through an ELGA Spectrum system. Borosilicate glass slide substrates were used for optical and electrical measurements. Various metals were investigated to establish electrical contact to the nanotubes, including silver paint (Agar Scientific, Electrodag 1415M), and thermally evaporated gold/aluminium and palladium.

Palladium electrodes separated by sub-micron gaps were fabricated on glass wafers using a modified version of a controlled undercutting method based on aluminium wet etching.[9] A description of the process can be found in the supporting information.

Current versus voltage measurements were taken over a range of temperatures (80 K – 350 K) in an Oxford Instruments OptistatDN cryostat controlled by an Oxford Instruments ITC 5035 temperature controller. A Keithley 2635A sourcemeter was used to record the data.

Atomic force microscopy images were obtained using a Digital Instruments Nanoscope E scanning probe microscope, operating in contact mode, or a Digital Instruments NanoMan II, in tapping mode. Scanning electron microscopy (SEM) images were measured in the immersion mode using an FEI Helios Nanolab 600 microscope. This equipment also allowed energy-dispersive X-ray spectroscopy (EDX) to be undertaken on the samples. Optical absorption spectra were gathered for SWCNTs in solution and as-deposited on glass substrates using a Shimadzu UV-3600 spectrometer. A Rudolph Research AutoEL-IV ellipsometer was used to measure film thicknesses and refractive indices at wavelengths of 633 nm and 546 nm.

Results and Discussion

Isotherms and Langmuir-Blodgett Deposition

Figure 1 shows a series of surface pressure versus area isotherms for semiconducting carbon nanotubes, showing the influence of the amount of material spread on the surface and the addition of methanol to the subphase. The data obtained for metallic nanotubes were very similar and are therefore not shown. The 'generic' isotherm (represented by the 0.005 ml curve) shows an expanded region, up to around 1 mN m^{-1} and then a constant pressure plateau. Following this, there is a relatively pronounced transition into a more condensed phase, which exhibits an almost linear increase in pressure up to approximately 10 mN m^{-1}. This suggests some organisation in the floating layer, with the nanotubes (or bundles of nanotubes) packing together on the surface. There is then a steady increase in surface pressure up to 14 mN m^{-1}, which is achieved at the minimum trough area of 20 cm^2. The rate of increase in surface pressure does reduce towards the minimum trough area, signifying that the maximum pressure generated by the nanotube layer has been reached.

If the isotherm generated from 0.015 ml of material is compared with the generic isotherm (0.005 ml), at first sight it appears very different. However, due to the increase in the amount of starting material, the isotherm has simply been shifted to the right, so the extended plateau region has disappeared and the more organized condensed phase is immediately observed. Interestingly, the rate of surface pressure increase is less rapid than that for the lower amount of material, possibly due to the formation of large aggregates on the subphase surface. These will reduce the ability of the nanotubes to organize and pack tightly on the surface. When even more starting material is used, a significantly higher starting pressure is observed (data for 0.1 ml), implying that there is already a film of nanotubes covering the surface of the water and reducing the surface tension (thereby increasing the surface pressure). As this film is compressed, there is little structure evident in the isotherm and there are no identifiable phase changes, or indeed a significant increase in surface pressure. We suggest that the floating SWCNT film is now in the form of relatively large aggregates on the water surface. These are unable to organize and pack tightly together as the tubes appear to do when smaller amounts of material are used.

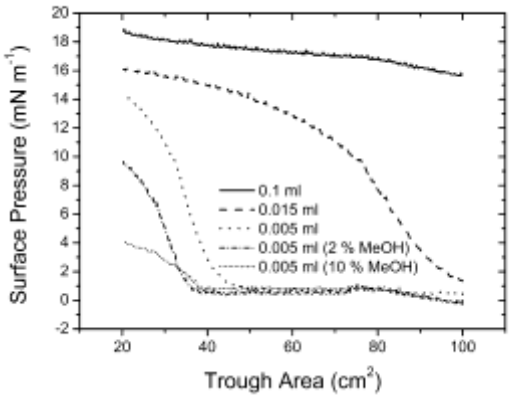

Figure 1. Surface pressure versus area isotherms for semiconducting carbon nanotubes, showing the influence of the volume of material spread and the addition of methanol to the

subphase. Subphase, pure water (pH = 5.8 ± 0.1 temperature = 20 ± 1˚C). Barrier compression rate = 0.5 mm s^{-1}.

Figure 1 also shows the effect of adding methanol to the pure water subphase. This approach has been used successfully to aid the spreading and LB transfer of phthalocyanine compounds.[10] On addition of 2 % (by volume) of methanol, the isotherm is noticeably changed. The overall surface pressure is reduced from a maximum of 14 mN m^{-1} to 10 mN m^{-1}. The transition point has also been shifted to the left (lower trough area) giving a smaller 'area per molecule' value. Addition of alcohol to water is known to cause a reduction in its surface tension; the decrease in maximum pressure observed in the nanotube layers corresponds approximately to the decrease caused by the addition of methanol.[11] When more methanol is added, 10 % (by volume), the maximum pressure falls even further to 4 mN m^{-1}, however the transition area, from expanded to condensed regions remains roughly the same, suggesting that the size of nanotube bundles had reached a minimum with the addition of 2 % methanol.

Using 'classical' LB organic compounds, for example long-chain fatty acids and their salts, a monomolecular layer can be formed at the air/water interface under appropriate conditions. This is then transferred to a substrate during the vertical LB deposition process as a complete film (e.g. like a carpet). Because of the rope-like and highly hydrophobic nature of the nanotubes, it is unlikely that perfect floating monomolecular layers are formed on the water surface. The floating film will almost certainly be more than a monolayer in thickness in parts and also contain gaps where no CNT material is present. In the forthcoming discussion, these layers will simply be referred to as 'floating layers', to avoid confusion with true monolayers.

For LB deposition, the floating SWCNT layers were held at a constant pressure in the steepest region of the pressure versus area isotherm. This was in the range 7 mN m^{-1} to 15

mN m^{-1}, depending on the amount of material spread and the quantity of methanol added to the subphase. Within this range of control pressures, the floating layer was generally stable, enabling film transfer. All of the nanotube materials used exhibited Z-type deposition on both hydrophilic and hydrophobic glass, i.e. deposition only occurring when the substrate was withdrawn through the floating layer. The addition of methanol to the subphase improved the film deposition, particularly in the case of the semiconducting nanotubes.

LB Film Morphology

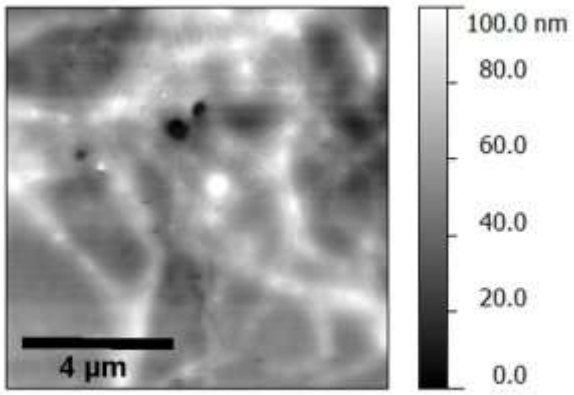

Figure 2. AFM image (tapping mode) of an as-deposited 5-layer SWCNT-S LB network on palladium.

Following LB deposition, inspection using the atomic force microscope revealed that semiconducting nanotubes appeared to be coated with a 'residue.' Figure 2 shows a typical AFM image of the film structure. The residue could be washed off using propanol followed by acetone; however a significant proportion of the tubes was also lost during this process. Annealing for 30 minutes at 150 °C also removed the residue (observed optically) and left more of the nanotube network intact (giving rise to a significantly higher conductivity through the network). It is thought that the surface coating was the remains of the surfactant

used during the separation process. Indeed, scanning electron microscope (SEM) studies and energy dispersive X-ray (EDX) spectra showed the presence of sodium deposits before washing and annealing, supporting this theory. Langmuir-Blodgett layers of the metallic nanotubes showed a similar residue. However, washing with methanol *before* dispersion in chloroform helped to remove this. This additional washing step did not help in cleaning the semiconducting nanotubes. The shape of the isotherm of the washed metallic material was similar to that of the unwashed material; however a higher surface pressure could be achieved.

The AFM images in Figure 3 show 5-layer LB films deposited on palladium following annealing at 150 °C for 30 minutes. These images are much sharper than that of Figure 2, revealing clear bundles of CNTs with no evidence of additional material. Both materials (SWCNT-S and SWCNT-M) deposited well over the entire area of the substrate, with the AFM images above showing typical regions. The films are in the form of networks of nanotube ropes. As can be seen in Figure 3(a), the metallic nanotubes appear to be in larger bundles and the coverage does not appear to be quite as uniform as the semiconducting nanotubes. A relevant observation made during the make-up of the spreading solutions was that, although both solutions were made up to the same concentration (~ 0.02 mg ml^{-1}), the metallic nanotubes did not appear to disperse as efficiently as the semiconducting tubes (Figure 3(b)). This is reinforced by the AFM images of the much more delicate structure to the ropes of SWCNT-S. The thickness the LB films can be estimated from the AFM data, giving an average layer thickness of 3 ± 1 nm for both types of film. Ellipsometry experiments, averaged over measurements at 633 nm and 546 nm, gave a layer thickness of 2 nm per layer for the semiconducting LB films. This smaller thickness value is probably related to the optical measurement method, which provides data that are representative of a surface not completely covered by carbon nanotubes, i.e. a CNT/air mixture. The

ellipsometry measurements also provided refractive index values (assuming a non-absorbing film) for the semiconducting LB networks: 2.26 at 633 nm, and 1.75 at 546 nm. Ellipsometry measurements for the metallic LB networks gave an average layer thickness of 1 nm per layer, this value is representative of a sparse network. The lower thickness value for the metallic CNTs is consistent with the poor LB deposition. Refractive index values for the metallic LB networks were: 1.85 at 633 nm, and 2.85 at 546 nm.

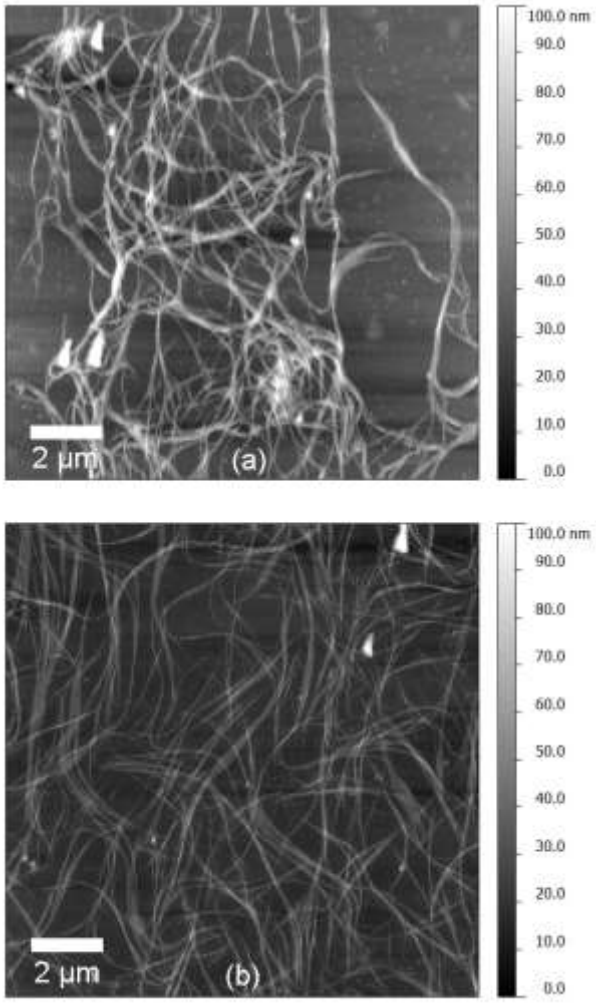

Figure 3. AFM images (contact mode) of (a) a 5-layer SWCNT-M LB network (b) a 5-layer SWCNT-S LB network. In both cases, the substrate is palladium and the films have been annealed at 150 °C for 30 minutes.

Figure 4 shows the absorption spectra across a wavelength range 400 nm – 1600 nm for 14-layer SWCNT-S and SWCNT-M LB films. Unsorted carbon nanotubes show relatively featureless absorption curves, with a general increase in absorption towards shorter wavelengths.[1] The separated materials show clear differences in their spectra, with absorption maxima at ~400 nm and ~1050 nm for semiconducting nanotubes, and maxima at ~400 nm and ~700 nm for the metallic nanotubes. These values agree with those reported in the literature.[8]

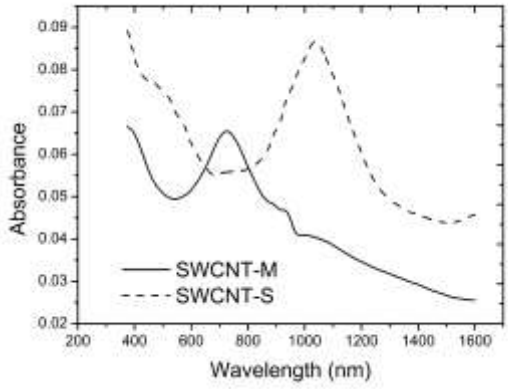

Figure 4. Optical absorbance for 14-layer SWCNT-S and SWCNT-M LB films.

Electrical Conductivity

Contact Effects

Palladium was the preferred electrode material in our experiments. In common with other reports, this metal formed the most reliable electrical contacts.[12,13] Measurements over

electrode spacings of 220 nm and 2 mm on the same network revealed that the current, measured at a fixed voltage, was inversely proportional to the gap between the electrodes, suggesting that contact effects were not dominant. Experiments were also undertaken using aluminium contacts. In these cases, the current versus voltage characteristics were non linear, indicating the presence of potential energy barriers at the contact/nanotube interfaces. The thermal annealing step, introduced after the LB deposition process to remove organic contamination from the SWCNTs (see section above), also improved the contact between the nanotubes and the electrodes. To investigate the conductivity across single nanotubes or bundles of tubes (rather than across a network of nanotubes), electrodes with sub-micron spacing were fabricated as described in the Experimental section. An AFM image of two bundles of SWCNT-S tubes across a gap of approximately 220 nm is shown in Figure 5.

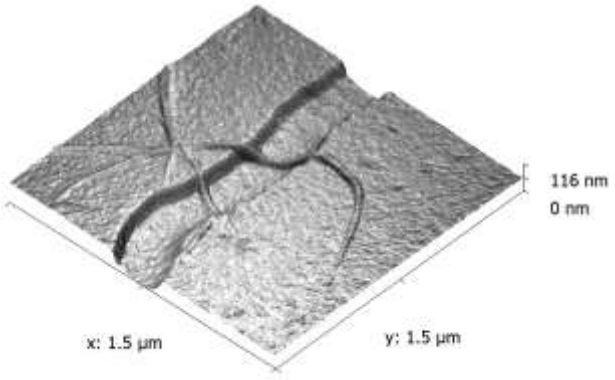

Figure 5. AFM image (tapping mode) of a single LB layer of SWCNT-S showing two bundles of SWCNT-S bridging a pair of palladium electrodes on glass.

Figure 6 shows the current, *I*, versus voltage, *V*, characteristics for our nanotube LB networks deposited on palladium sub-micron electrodes. This also shows the effect of thermal annealing at 150 °C for 30 minutes. In their as-deposited state, the SWCNT-S reveal little conductivity, but following annealing the current increases to several mA. The metallic

nanotubes exhibit good conductivity as deposited, but with some non-linearity in their *I-V* response. After annealing, the current increases to a maximum of around 40 mA at 1 V; the linearity of the *I-V* characteristic has also improved. The results suggest that good ohmic contacts are established to the LB nanotube networks following annealing. The optimum anneal time was 30 min to 90 minutes, with little improvement in the conductivity for longer times. The following sections describe detailed studies of the electrical conductivity of LB films of both the SWCNT-S and SWCNT-M materials.

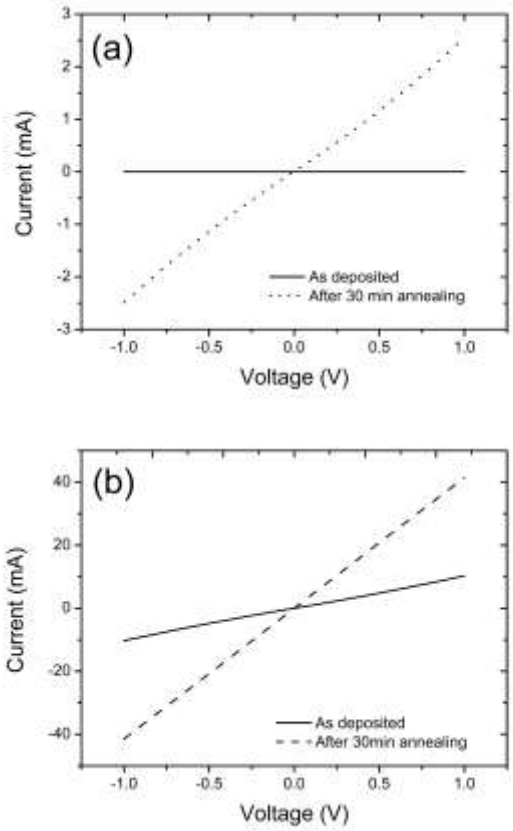

Figure 6. Current versus voltage characteristics for (a) a 5-layer SWCNT-S LB network and (b) a 5-layer SWCNT-M LB network, both with palladium sub-micron electrodes. The figures also show the effect of annealing at 150 °C for 30 minutes.

Semiconducting SWCNTs

Figure 7 shows the *I-V* behavior, over the temperature range 80 K to 350 K, for a SWCNT-S network (5 LB layers) deposited on glass with 220 nm-spaced palladium electrodes. The film resistance increases at lower temperatures, typical of a semiconducting material. Above 150 K, the current versus voltage response is almost linear. However, the *I-V* curves become increasingly non-linear as the temperature is reduced.

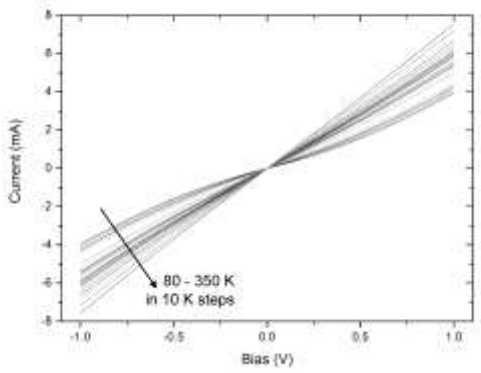

Figure 7. Current versus voltage characteristics for a 5-layer SWCNT-S LB network at varying temperatures on palladium electrodes, with a spacing of 220 nm.

Figure 8(a) shows that the applied voltage affects the resistance of the SWCNT-S thin film network; the resistance data are shown for two different values of applied voltage (1 V and 0.08 V). This plot is consistent with that shown in Figure 7, revealing an increasing non-linearity in the current versus voltage characteristics below 150 K. The same data are shown in the form of logarithm (current) versus the reciprocal of temperature in Figure 8(b); note the different ordinate scale corresponding to the two applied voltages. These Arrhenius plots are not in the form of single straight lines, as might be expected for a crystalline semiconductor

exhibiting intrinsic conductivity, or extrinsic conductivity dominated by a single impurity level. If the classical single crystal semiconductor model is appropriate, there would appear to be multiple impurity levels, or perhaps a continuum of levels, within the band gap of the carbon nanotube. A range of activation energies is apparent from Figure 8(b) with values between 1 meV to 41 meV. Typical figures reported in the literature tend to range from about 29 meV for individual un-doped nanotubes[14] to 10-20 meV for layer-by-layer nanotube films.[15]

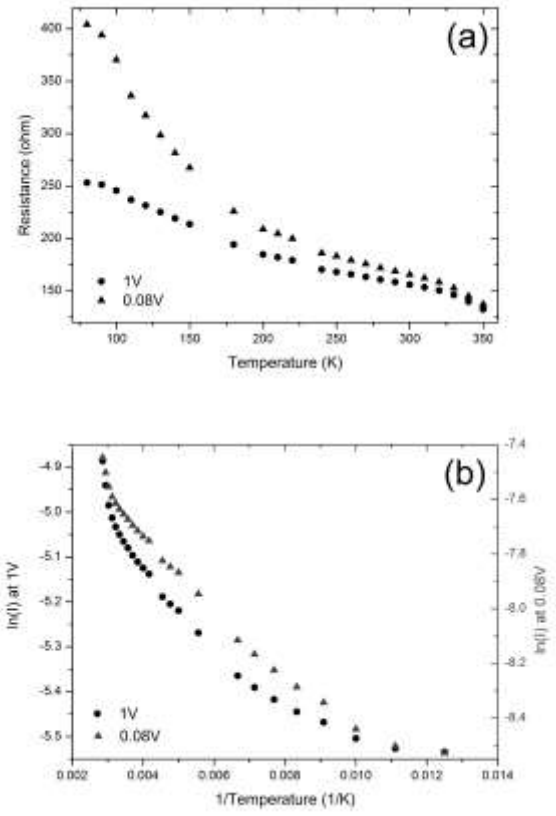

Figure 8. (a) Resistance versus temperature plot for a 5-layer SWCNT-S LB network at two different voltages, with an electrode spacing of 220 nm. (b) Arrhenius plots for the same data.

There are a number of different physical processes that could account for the electrical conductivity of our semiconductive nanotube networks. These have been discussed in the

literature.[14-16] Assuming that the conductivity is dominated by bulk rather than surface effects (evidenced by our experiments with different electrode spacings), possible conductivity mechanisms that have been considered to explain the electrical conduction in unsorted (i.e. mixed semiconducting and metallic) carbon nanotube films include quantum mechanical tunnelling between the individual tubes and variable range hopping.

The data shown in Figure 8 suggest that, at low temperatures, the conductivity is dependent on the applied electric field. Therefore, one mechanism that should be considered is that of Poole-Frenkel conduction. This is a bulk-limited process that operates at high electric fields ($> 10^6$ V m^{-1}) in which the conduction is determined the energy barriers surrounding charged traps. The dependence of current on the electric field, F, is given by

$$I = AF \exp\left(\frac{\beta_{PF} F^{\frac{1}{2}}}{kT} - \varphi\right) \qquad (1)$$

where A is a constant, φ is a constant related to the trap depth and β_{PF} is the Poole-Frenkel constant, given by

$$\beta_{PF} = \left(\frac{e^3}{\pi \varepsilon_0 \varepsilon_r}\right)^{\frac{1}{2}} \qquad (2)$$

where ε_0 is the permittivity of free space and ε_r is the relative permittivity of the medium.

Our previous work has suggested that Poole-Frenkel conduction provides a good explanation for the conductivity of SWCNT (unsorted) thin films deposited by electrostatic-layer-by-layer deposition.[15]

The variable range hopping model gives a conductance, G, dependence on temperature of the form[14]

$$G(T) = G_0 exp\left[-\left(\frac{T_0}{T}\right)^{1+d}\right] \qquad (3)$$

where G_0 and T_0 are constants and d refers to the number of dimensions (in this case 2).

Figure 9 shows our data for the SWCNT-S networks plotted to reveal Poole-Frenkel ($\ln(I/V)$ versus $V^{1/2}$) or variable range hopping ($\ln(I)$ versus $T^{-1/3}$) conductivity. Poole-Frenkel conduction (Figure 9(a)) seems to provide the better fit to the experimental data, particularly at temperatures below 150 K and values of applied voltage greater than 0.25 V (corresponding to an applied electric field of 1.7×10^6 V m^{-1}). In the case of variable range hopping, Figure 9(b), there appears to be a deviation away from the model at both higher and lower temperatures, suggesting other conduction processes could be at work.

Assuming that the conductivity is determined by the Poole-Frenkel process and using equations (1) and (2), a value for relative permittivity was calculated to be 984 at 80 K. This is significantly higher than reported in our previous work, with values between 6 and 22.[6] Our ellipsometry data reveal 'normal' refractive index values at optical frequencies (2.26 at 633 nm, and 1.75 at 546 nm, in the case of the semiconducting LB networks). However, the permittivity extracted from the Poole-Frenkel fitting is consistent with reports in the literature of very high dielectric constants for composite nanotube-polymer networks, with values up to 9000 at low frequencies.[17,18] This is attributed to the nanotubes being in very close proximity to each other but remaining insulated by thin regions of polymer within the film (i.e. close to the percolation threshold). The film as a whole can then be regarded as a micro capacitor network leading to the very high values of permittivity due to a build up of interface charge

by Maxwell-Wagner polarization. It is likely that our CNT networks, deposited on an insulating (glass) substrate, act in a similar manner, giving enhanced permittivity values at low frequencies.

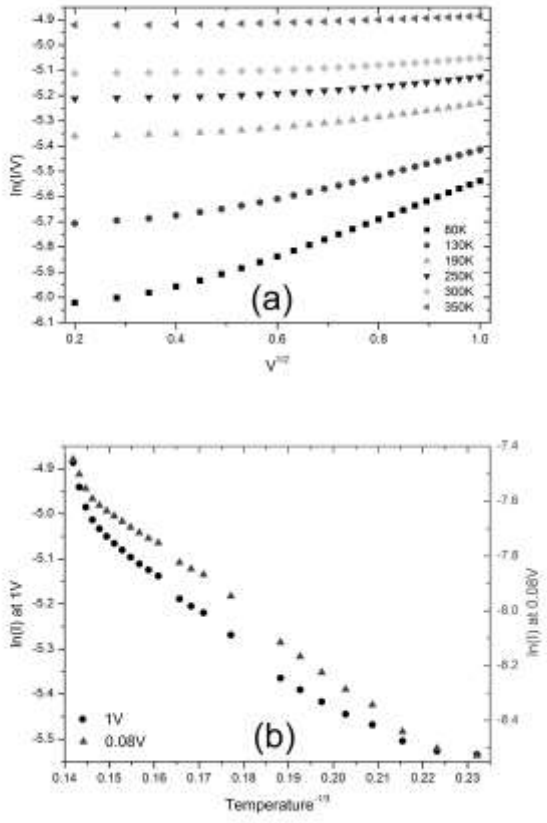

Figure 9. (a) Poole-Frenkel voltage dependence at fixed temperatures for a 5-layer SWCNT-S LB network deposited on glass with palladium electrodes, spacing 220 nm. (b) Variable range hopping (in 2 dimensions) plot for the same SWCNT-S network.

Across much larger electrode gaps (2 mm) the current versus voltage characteristics of all our SWCNT-S thin film networks were linear. Clearly, in these instances, it is the conductivity of the nanotube networks, rather than the conductivity of individual bundles of tubes (e.g. as shown in Figure 5) that is being measured. A typical set of *I-V* characteristics at different temperatures is shown in Figure 10 (a), the inset shows the resistance versus

temperature for two applied voltages. No voltage-dependent behaviour is evident, in contrast to the results obtained with sub-micron electrode separations, where we suggest that Poole-Frenkel conductivity is dominant. Figure 10 (b) shows an Arrhenius plot for the same data, the activation energies range from 3.7 meV to 34.6 meV, similar to the values obtained from Figure 8(b).

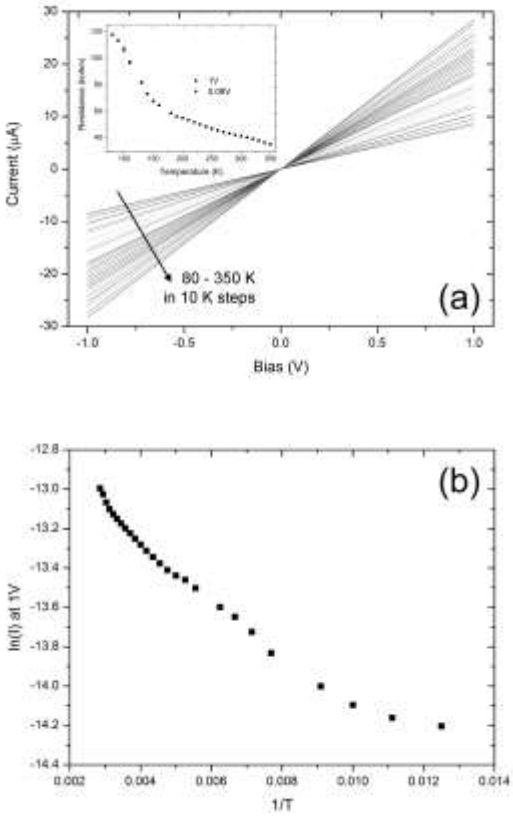

Figure 10. (a) Current versus voltage plots for a 5-layer SWCNT-S LB network at varying temperatures on palladium electrodes, with a spacing of 2 mm. The inset shows a resistance versus temperature plot at two different voltages. (b) Arrhenius plot for the same data.

Metallic SWCNTs

The current versus voltage curves for a 5-layer SWCNT-M LB film network over the temperature range 80 – 350 K are shown in Figure 11; the spacing of the palladium electrodes was 220 nm. In contrast to the data for SWCNT-S material (Figure 7), the *I-V* curves are linear for all the measurement temperatures. Furthermore, the resistance of the network decreases with decreasing temperature, as shown in the inset to Figure 11. This is as expected for a metal. The resistance versus temperature relationship can be approximated by

$$R(T) = R_0[1 + \alpha(T - T_0)] \qquad (4)$$

where R_0 and T_0 are a fixed resistance and temperature (in this case 25.4 ohms at 300 K), and α represents the temperature coefficient of resistance, 0.001 K^{-1} in this case. This figure is of the same order of magnitude to published work, e.g. 0.0026 K^{-1}.[19]

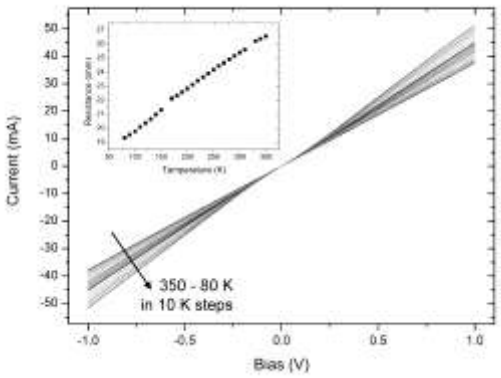

Figure 11. Current versus voltage plots for a 5-layer SWCNT-M LB network at varying temperatures on palladium electrodes, with a spacing of 220 nm. The inset shows the resistance versus temperature.

Conclusions

Thin networks of sorted semiconducting and metallic single-walled carbon nanotubes have been deposited by Langmuir-Blodgett deposition without the intentional addition of surfactants. By using palladium metal electrodes with a thermal annealing step after deposition, ohmic contacts were formed to both the SWCNT-S and SWCNT-M thin film networks. Electrical conductivity measurements, taken over the temperature range 80 – 350 K, have suggested that Poole-Frenkel conduction is the dominant conduction mechanism in the SWCNT-S networks across small electrode separations (220 nm) and at temperatures below 150 K. This electric field dependent conductivity was not evident in the networks across larger gaps (2 mm). For metallic nanotubes, a simple linear relationship between conduction and temperature was found, with an increasing conductivity with decreasing temperature.

Acknowledgments

One of us (MKM) would like to thank the School of Engineering and Computing Sciences for the provision of a studentship.

Supporting Information Available: <Fabrication process for sub-micron gap palladium electrodes.> This material is available free of charge via the Internet at http://pubs.acs.org.

References

1. Hu, L.; Hecht, D. S.; Grüner, G. Carbon nanotube thin films: fabrication, properties and applications. *Chem. Rev.* **2010,** *110* (10), 5790-5844.

2. Kim, Y.; Minami, N.; Zhu, W.; Kazaoui, S.; Azumi, R.; Matsumoto, M. Langmuir-Blodgett films of single-wall carbon nanotubes: layer-by-layer deposition and in-plane orientation of tubes. *Jpn. J. Appl. Phys.* **2003,** *42,* 7629-7634.

3. Giancane, G.; Ruland, A.; Sgobba, V.; Manno, D.; Serra, A.; Farinola, G. M.; Omar, O. H.; Guldi, D. M.; Valli, L. Aligning single-walled carbon nanotubes by means of Langmuir-Blodgett film deposition: optical, morphological, and photo-electrochemical studies. *Adv Funct. Mater.* **2010,** *20,* 2481-2488.

4. Guo, Y.; Minami, N.; Kazaoui, S.; Peng, J.; Yoshida, M.; Miyashita, T. Multi-layer LB films of single-wall carbon nanotubes. *Physica B* **2002,** *323,* 235-236.

5. Lee, J.-H.; Kang, W.-S.; Choi, B.-S.; Choi, S.-W.; Kim, J.-H. Fabrication of carbon nanotube AFM probes using the Langmuir-Blodgett technique. *Ultramicroscopy* **2008,** *108,* 1163-1167.

6. Massey, M. K.; Pearson, C.; Zeze, D. A.; Mendis, B.; Petty, M. C. The electrical and optical properties of orientated Langmuir-Blodgett films of single-walled carbon nanotubes. *Carbon* **2011,** *49,* 2424-2430.

7. Venet, C.; Pearson, C.; Jombert, A. S.; F, M. M.; Zeze, D. A.; Petty, M. C. The morphology and electrical conductivity of single-walled carbon nanotube thin films prepared by the Langmuir-Blodgett technique. *Colloids and Surfaces A: Physicochem. Eng. Aspects* **2010,** *354,* 113-117.

8. Green, A. A.; Hersam, C. Colored semitransparent conductive coatings of monodisperse metallic single-walled carbon nanotubes. *Nano Lett.* **2008,** *8* (5), 1417-1422.

9. Rosamond, M. C.; Gallant, A. J.; Petty, M. C.; Kolosov, O.; Zeze, D. A. A versatile nanopatterning technique based on controlled undercutting and liftoff. *Adv. Mater.* **2011,** *23* (43), 5039-5044.

10. Roberts, G. G.; Petty, M. C.; Baker, S.; Fowler, M. T.; Thomas, N. J. Electronic devices incorporating stable phthalocyanine Langmuir-Blodgett films. *Thin Solid Films* **1985,** *132,* 113-123.

11. Vázquez, G.; Alvarez, E.; Navaza, M. J. Surface tension of alcohol + water from 20 to 50 C. *J. Chem. Eng. Data* **1995,** *40,* 611-614.

12. Chen, Z.; Appenzeller, J.; Joachim, K.; Lin, Y.; Avouris, P. The role of metal-nanotube contact in the performance of carbon nanotube field-effect transistors. *Nano Lett.* **2005,** *5* (7), 1497-1502.

13. Mann, D.; Javey, A.; Kong, J.; Wang, Q.; Dai, H. Ballistic transport in metallic nanotubes with reliable Pd Ohmic contacts. *Nano Lett.* **2003,** *3* (11), 1541-1544.

14. Skákalová, V.; Kaiser, A. B.; Woo, Y. -S.; Roth, S. Electronic transport in carbon nanotubes: from individual nanotubes to thin and thick networks. *Phys. Rev. B* **2006,** *74,* 085403.

15. Jombert, A. S.; Coleman, K. S.; Wood, D.; Petty, M. C.; Zeze, D. A. Poole-Frenkel conduction in single wall carbon nanotube composite films built up by electrostatic layer-by-layer deposition. *J. Appl. Phys.* **2008,** *104,* 094503.

16. Yanagi, K.; Udoguchi, H.; Sagitani, S.; Oshima, Y.; Takenobu, T.; Kataura, H.; Ishida, T.; Matsuda, K.; Maniwa, Y. Transport mechanisms in metallic and semiconducting single-wall carbon nanotube networks. *ACS Nano* **2010,** *4* (7), 4027-4032.

17. Yuan, J.-K.; Yao, S.-H.; Dang, Z.-M.; Sylvestre, A.; Genestoux, M.; Bai, J. Giant dielectric permittivity nanocomposites: realizing true potential of pristine carbon nanotubes in polyvinylidene fluoride matrix through an enhanced interfacial interaction. *J. Phys. Chem* **2011,** *115,* 5515-5521.

18. Zhao, X.; Koos, A. A.; Chu, B. T. T.; Johnston, C.; Grobert, N.; Grant, P. S. Spray deposited fluoropolymer/multi-walled carbon nanotube composite films with high dielectric permittivity at low percolation threshold. *Carbon* **2009,** *47,* 561-569.

19. Pop, E.; Mann, D. A.; Goodson, K. E.; Dai, H. Electrical and thermal transport in metallic single-wall carbon nanotubes on insulating substrates. *J. Appl. Phys.* **2007,** *101,* 093710.

Table of contents only